BRAIN
ORIGINAL ARTICLE

HLA-DQB1*05 subtypes and not DRB1*10:01 mediates risk in anti-IgLON5 disease

Selina M. Yogeshwar,[1,2,3] Sergio Muñiz-Castrillo,[1] Lidia Sabater,[4] Vicente Peris-Sempere,[1] Vamsee Mallajosyula,[5] Guo Luo,[1] Han Yan,[1] Eric Yu,[1] Jing Zhang,[1] Ling Lin,[1] Flavia Fagundes Bueno,[1] Xuhuai Ji,[6] Géraldine Picard,[7,8] Véronique Rogemond,[7,8] Anne Laurie Pinto,[7,8] Anna Heidbreder,[9] Romana Höftberger,[10] Francesc Graus,[11] Josep Dalmau,[11,12,13,14] Joan Santamaria,[11] Alex Iranzo,[11] Bettina Schreiner,[15,16] Maria Pia Giannoccaro,[17,18] Rocco Liguori,[17,18] Takayoshi Shimohata,[19] Akio Kimura,[19] Yoya Ono,[19] Sophie Binks,[20,21] Sara Mariotto,[22] Alessandro Dinoto,[22] Michael Bonello,[23] Christian J. Hartmann,[24,25] Nicola Tambasco,[26] Pasquale Nigro,[26] Harald Prüss,[2,27] Andrew McKeon,[28,29] Mark M. Davis,[5,30,31] Sarosh R. Irani,[21] Jérôme Honnorat,[7,8] Carles Gaig,[11] Carsten Finke[2,32] and Emmanuel Mignot[1]

Anti-IgLON5 disease is a rare and likely underdiagnosed subtype of autoimmune encephalitis. The disease displays a heterogeneous phenotype that includes sleep, movement and bulbar-associated dysfunction. The presence of IgLON5-antibodies in CSF/serum, together with a strong association with *HLA-DRB1*10:01~DQB1*05:01*, supports an autoimmune basis.

In this study, a multicentric human leukocyte antigen (HLA) study of 87 anti-IgLON5 patients revealed a stronger association with *HLA-DQ* than *HLA-DR*. Specifically, we identified a predisposing rank-wise association with *HLA-DQA1*01:05~DQB1*05:01*, *HLA-DQA1*01:01~DQB1*05:01* and *HLA-DQA1*01:04~DQB1*05:03* in 85% of patients. HLA sequences and binding cores for these three DQ heterodimers were similar, unlike those of linked DRB1 alleles, supporting a causal link to HLA-DQ. This association was further reflected in an increasingly later age of onset across each genotype group, with a delay of up to 11 years, while HLA-DQ-dosage dependent effects were also suggested by reduced risk in the presence of non-predisposing DQ1 alleles. The functional relevance of the observed HLA-DQ molecules was studied with competition binding assays. These proof-of-concept experiments revealed preferential binding of IgLON5 in a post-translationally modified, but not native, state to all three risk-associated HLA-DQ receptors. Further, a deamidated peptide from the Ig2-domain of IgLON5 activated T cells in two patients, compared with one control carrying *HLA-DQA1*01:05~DQB1*05:01*.

Taken together, these data support a HLA-DQ-mediated T-cell response to IgLON5 as a potentially key step in the initiation of autoimmunity in this disease.

1 Stanford Center for Sleep Sciences and Medicine, Stanford University School of Medicine, Stanford, CA 94305, USA
2 Department of Neurology and Experimental Neurology, Charité-Universitätsmedizin Berlin, Corporate Member of Freie Universität Berlin, Humboldt-Universität Berlin, 10117, Berlin, Germany
3 Einstein Center for Neurosciences Berlin, Charité—Universitätsmedizin Berlin, 10117 Berlin, Germany
4 Neuroimmunology Program, Fundació de Recerca Clínic Barcelona-Institut d'Investigacions Biomèdiques August Pi i Sunyer, Caixa Research Institute, Universitat de Barcelona, 08036, Barcelona, Spain

Received June 23, 2023. Revised October 09, 2023. Accepted January 21, 2024. Advance access publication March 1, 2024

5 Institute for Immunity, Transplantation, and Infection, Stanford University School of Medicine, Stanford, CA 94305, USA
6 Human Immune Monitoring Center, Institute for Immunity, Transplantation, and Infection, Stanford University School of Medicine, Stanford, CA 94305, USA
7 French Reference Center on Paraneoplastic Neurological Syndrome and Autoimmune Encephalitis, Hospices Civils de Lyon, 69677, Lyon, France
8 Institut MeLiS INSERM U1314/CNRS UMR 5284, Université Claude Bernard Lyon 1, 69372 Lyon, France
9 Kepler University Hospital, Department of Neurology, Johannes Kepler University, 4020 Linz, Austria
10 Division of Neuropathology and Neurochemistry, Department of Neurology, Medical University of Vienna, 1090 Vienna, Austria
11 Neurology Service, Hospital Clínic of Barcelona, Biomedical Research Institute (IDIBAPS), 08036 Barcelona, Spain
12 Catalan Institution for Research and Advanced Studies (ICREA), 08010 Barcelona, Spain
13 Department of Neurology, University of Pennsylvania, Philadelphia, PA 19104, USA
14 Spanish National Network for Research on Rare Diseases (CIBERER), 28029 Madrid, Spain
15 Department of Neurology, University Hospital Zurich, 8091 Zurich, Switzerland
16 Institute of Experimental Immunology, University of Zurich, 8057 Zurich, Switzerland
17 IRCCS Istituto delle Scienze Neurologiche di Bologna, UOC Clinica Neurologica, 40139 Bologna, Italy
18 Dipartimento di Scienze Biomediche e Neuromotorie, Università di Bologna, 40100 Bologna, Italy
19 Department of Neurology, Gifu University Graduate School of Medicine, 501-1194 Gifu, Japan
20 Oxford Autoimmune Neurology Group, Nuffield Department of Clinical Neurosciences, University of Oxford, Oxford OX3 9DU, UK
21 Department of Neurology, Oxford University Hospitals NHS Foundation Trust, John Radcliffe Hospital, Oxford OX3 9DU, UK
22 Neurology Unit, Department of Neurosciences, Biomedicine, and Movement Sciences, University of Verona, 37124 Verona, Italy
23 Department of Neurology, The Walton Centre NHS Foundation Trust, L9 7LJ, Liverpool, UK
24 Department of Neurology, Medical Faculty and University Hospital Düsseldorf, Heinrich Heine University Düsseldorf, 40225 Düsseldorf, Germany
25 Institute of Clinical Neuroscience and Medical Psychology, Medical Faculty and University Hospital Düsseldorf, Heinrich Heine University Düsseldorf, 40225 Düsseldorf, Germany
26 Movement Disorders Center, Neurology Department, Perugia General Hospital and University of Perugia, 06156 Perugia, Italy
27 German Center for Neurodegenerative Diseases (DZNE) Berlin, 10117 Berlin, Germany
28 Department of Laboratory Medicine and Pathology, Mayo Clinic, Rochester, MN 55905, USA
29 Department of Neurology, Mayo Clinic, Rochester, MN 55905, USA
30 Department of Microbiology and Immunology, Stanford University School of Medicine, Stanford, CA 94305, USA
31 Howard Hughes Medical Institute, Stanford University School of Medicine, Stanford, CA 94305, USA
32 Berlin Center for Advanced Neuroimaging, Charité—Universitätsmedizin Berlin, Corporate Member of Freie Universität Berlin and Humboldt-Universität zu Berlin, 10117 Berlin, Germany

Correspondence to: Emmanuel J. M. Mignot
Stanford Center for Sleep Sciences and Medicine, Stanford University School of Medicine
3165 Porter Drive, Palo Alto, CA 94304, USA
E-mail: mignot@stanford.edu

Keywords: autoimmunity; autoimmune encephalitis; HLA; T cell; IgLON5

Introduction

Anti-IgLON5 disease is a recently described autoimmune syndrome, with distinctive and polymorphic clinical features.[1] It affects both sexes equally and has a late age of onset, with a mean age at diagnosis of >60 years.[2] Symptoms may include a complex form of sleep disorder, with REM/non-REM parasomnia, sleep apnoea, and stridor, gait and other movement abnormalities, as well as bulbar and cognitive impairment. All patients are positive for serum, and in most cases, CSF autoantibodies targeting the extracellular domain of IgLON5.[2] Early on in the disease, CSF pleocytosis is observed, consistent with CNS inflammation.[2] Also, a neurodegenerative biology is supported by neuropathological[3,4] and PET[5] studies, showing the accumulation of hyperphosphorylated tau in the brains of patients. However, neuropathological studies indicate rare cases may present without a tauopathy.[6,7]

A clinical diagnosis can be difficult, as late onset and symptomatology overlap with that of neurodegenerative disorders and the only very recent description of this condition suggests it remains likely under-recognized. Importantly, early and aggressive immunotherapy can stabilize or even ameliorate symptoms, although treatment remains poorly effective in >50% of patients.[8] However, a better understanding of the underlying pathophysiology of this devastating disorder may pave the way for alternative and improved therapeutics.

IgLON5 belongs to a family of five highly homologous cell surface immunoglobulin-like cell adhesion molecules that are widely expressed in the CNS[9,10] and myoblasts,[11] whereby murine IgLON5 was found to be expressed at higher levels in the brainstem,

thalamus, ventral striatum and olfactory bulb,[12] thus mirroring tauopathy-affected distribution.[3] Studies of cultured rat hippocampal neurons[13] and human neural stem cells[14] have shown that IgGs from patient sera can lead to disrupted cytoskeletal organization and neurodegenerative changes, while *in vivo* evidence from mouse models further supports disruptions to synaptic homeostasis and irreversible neuronal damage.[15]

Altogether, these studies suggest that autoimmunity operates upstream of neurodegeneration, triggering neuronal structural damage and tau accumulation later in the course of the disease. Identification of key, early autoimmune pathways involved in triggering the generation of cytotoxic tau and neurodegeneration, therefore, may provide both early therapeutic targets for the successful treatment of this disorder and, beyond that, provide insights into crucial autoimmune-neurodegenerative mechanisms that are relevant beyond this disease too.

An autoimmune origin for the disease is further supported by a unique human leukocyte antigen (HLA) class II association,[1,16] similar to those found in other autoimmune diseases such as coeliac disease (*DQ2*),[17] rheumatoid arthritis (*DR4*)[18] and, in CNS conditions, narcolepsy (*DQ0602*)[19] and other autoimmune encephalitis syndromes associated with LGI1 and CASPR2 antibodies.[20] HLA class II molecules play a key role in initiating and driving autoimmunity by presenting (auto)antigens to $CD4^+$ T cells, leading to subsequent T- and B-cell activation.[21,22] However, T-cell contributions, and the precise HLA molecules involved in T-cell activation, have received limited attention. Although the mechanisms underlying autoreactivity are poorly understood, molecular mimicry with foreign antigens is strongly suggested in some diseases, such as Epstein-Barr virus in multiple sclerosis[23,24] or influenza in narcolepsy.[25,26] Interestingly, autoantigens are often post-translationally modified (PTM); for example, they are citrullinated in rheumatoid arthritis[18,27] or cryptically fused in type 1 diabetes,[28,29] in line with reduced negative selection for PTMs in the thymus.[30]

The objective of this study was to conduct an HLA-association analysis in a large sample of anti-IgLON5 disease patients to examine candidate autoimmune HLA-peptide binding and probe $CD4^+$ T-cell reactivity to candidate binders, thereby ultimately allowing us to disentangle triggers and key events in the pathophysiology of this disease.

Materials and methods

Participants

A total of 87 patients with anti-IgLON5 disease enrolled across Spain (51), Italy (2), France (18; French samples were banked in NeuroBioTec Hospices Civils de Lyon BRC, France, AC-2013-1867, NFS96-900), Germany (4), Switzerland (5), Brazil (1), Japan (1), USA (4) and the UK (1) were used (Table 1 and Supplementary Fig. 1). All patients were positive for IgLON5 autoantibodies in serum. Data from 44 of these patients were published previously[1,16,31-37] (Supplementary Table 1). A subset of 75 patients had DNA available for a genome-wide association study (GWAS); these were used for HLA analysis versus controls matched by ethnicity using principal component analysis (PCA; case control analysis). An additional 12 subjects had HLA typing and clinical data available; these were used in addition to the 75 to maximize power for analyses comparing symptoms across HLA type categories within anti-IgLON5 disease patients (phenotypic analysis) (Supplementary Fig. 1). Clinical data were collected from clinical records or assessed as previously described.[1,31]

Table 1 Description of patient cohort

Description of patient cohort	Frequency (%), number (*n*)
Data availability[a]	
Clinical data[b]	90% (78/87)
Full genotyping and HLA imputation	86% (75/87)
Full or partial 4-digit resolution typing	58% (50/87)
Full or partial 8-digit resolution typing	17% (15/87)
Demographic information	
Sex	
Male	56% (49/87)
Female	44% (38/87)
Age	
At disease onset	μ = 63.4 years (34–91 years)
At disease diagnosis	μ = 66.7 years (35–91 years)
Clinical presentation[b,c]	
Sleep disturbances	45% (32/71)
Bulbar symptoms	45% (32/71)
Movement disorders	32% (23/71)
Gait abnormalities	11% (8/71)
Neuromuscular abnormalities	11% (8/71)
Cognitive dysfunction	28% (20/71)
Dysautonomia	11% (8/71)
Other	9% (6/71)

[a]For information on overlap of data entities by patients, see Supplementary Fig. 1; for a detailed summary of data availability of all patients, see Supplementary Table 1.
[b]Clinical data were only analysed for patients with full HLA-typing or imputation available ($n = 71$).
[c]Major clinical classifications, see Gaig *et al.*[31] and Grüter *et al.*[2]

HLA and genotyping

DNA was available from 75 patients (Supplementary Fig. 1) and genotyped using the Affymetrix Precision Medicine Research Array (AKESOgen). All quality control and genotype single nucleotide polymorphism (SNP) operations such as creating Manhattan plots, zoom plots and using FINEMAP (Supplementary Fig. 2) were conducted using PLINK.[38] Genotypes with an imputation probability <0.3 were removed. Haplotypes were phased and merged using QCTOOL and imputed to 1000 Genome Phase III. Patients were matched to controls by PCA (Eucleadian distance-based measure[39]) at a 1:8 ratio from a set of 2503 controls, giving rise to 232 matched controls (1:3.1; Fig. 1A). HLA Genotype Imputation with Attribute Bagging (HIBAG)[40] was used to perform HLA imputation. Calls with a probability <0.75 ($n = 4$) were additionally HLA-typed using next-generation sequencing (NGS)[41-43] (Supplementary Figs 1 and 3). Prior 4-digit resolution HLA typing data were available from 50 patients. To further validate imputation, an additional 14 randomly selected participants were typed using 8-digit resolution NGS HLA genotyping (Supplementary Fig. 1 and Supplementary Table 1).

Statistical analyses

For genetic analyses, categorical variables are presented as percentages (%) and total number of subjects (*n*) for any group reported in brackets. For allele carrier frequencies, a generalized logistic model (GLM) was fit to each allele, controlled by the first three principal components. The analysis was repeated after conditioning for specific haplotypes, as previously described.[44] For haplotype analyses, a count of heterozygous and homozygous cases and controls was conducted, whereby controls were matched to cases by PCA (see earlier). χ^2 statistics and odds ratios (ORs) are reported. Age at disease onset between different HLA-carrier groups (Fig. 2) was compared using Mann–Whitney U-test, with data-points shown for all

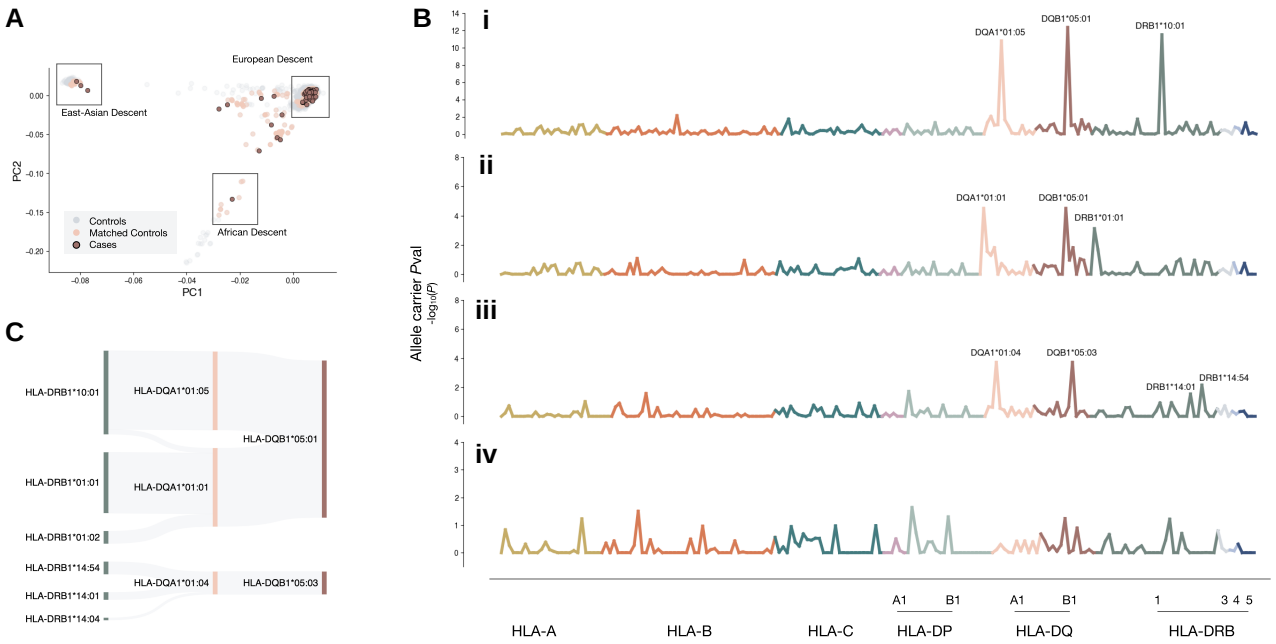

Figure 1 HLA-association with three conserved *HLA-DQ5* haplotypes. (**A**) The first two principal components (PC1, PC2) are shown to highlight the ethnic diversity of subjects included in the study. Cases were matched at a 1:8 ratio to controls from a set of 2503 controls by principal component analysis. [**B(i)**] HLA association of anti-IgLON5 disease across HLA class I and II is shown unconditioned, (**ii**) under conditioned exclusion of *HLA-DRB1*10:01*, (**iii**) *HLA-DRB1*10:01*, *HLA-DRB1*01:01* and *HLA-DRB1*01:02* and (**iv**) *HLA-DRB1*10:01*, *HLA-DRB1*01:01*, *HLA-DRB1*14:01*, *HLA-DRB1*14:54* and *HLA-DRB1*14:04*. (**C**) Sankey plot shows conservation of risk-associated *HLA-DRB1-DQA1-DQB1* haplotypes among cases.

groups together with a box plot showing interquartile range (IQR) mean and whiskers extending to the smallest and largest data-points within 1.5 times the IQR and violin plots showing data distribution. Total number *n* is reported for all clinical and demographic parameters. For peptide binding experiments, the mean of data and standard error of the mean (SEM) is shown for all data-points. All analyses were performed using R and Python. Significance levels were set at $^{*}P < 0.05$ and $^{**}P < 0.01$. All *P*-values are false discovery rate (FDR) corrected.

Transfection and purification of HLA class II monomers

Plasmids encoding HLA-DQA1*01:01, HLA-DQA1*01:04, HLA-DQA1*01:05, HLA-DQB1*05:01, HLA-DQB1*05:03, HLA-DRA1*01:01 and HLA-DRB1*10:01 were purified according to manufacturer's instructions (Qiagen, Cat. No. 12662) and transfected into Sf9 cells using BestBac2.0 (Cat. No. 91-002, Expression Systems), with P0 stock virus harvested after 5 days. Successful transfection was confirmed using a Baculovirus Titering Kit (Cat. No. 97-101, Expression Systems) and flow cytometric analysis. Following this, 100 ml of Sf9 cells were seeded at a concentration of $\sim 1 \times 10^6$ cells/ml together with 100 µl of P0 in a 27°C shaking incubator. On Day 3, cells were resuspended in fresh medium (Sf-900™ III SFM; Thermo Scientific, Cat. No. 12658019), supplemented with 1% GlutaMAX™ (Thermo Fisher Scientific, Cat. No. 35050061) and 10% fetal bovine serum (FBS; Gibco, Cat. No. 26140079) and subsequently set down for 7 days more. P1 was harvested and tested using a Baculovirus Titering Kit (Cat. No. 97-101, Expression Systems), flow cytometric analysis and a Lentivirus Titer Kit (Cell Biolabs, Cat. No. VPK-107).

Amplification of virus titres was repeated for four to six generations and tested using a minimum protein expression protocol, whereby 300 ml of Hi5 cells at a density of 2×10^6 cells/ml were incubated with 1.5 ml of amplified P virus at 27°C in a shaking incubator for 3 days. Following the 3-day incubation, the supernatant was harvested and proteins purified using a Protino Ni-NTA Agarose for His-tag protein purification kit (Machery-Nagel, Cat. No. 745400.100). The eluted protein was mixed with 4× Laemmli buffer (Bio-Rad, Cat. No. 1610747) and boiled for 10 min at 95°C before loading onto a mini-PROTEAN® TGX® precast gel for SDS-PAGE (Bio-Rad, Cat. No. 4561093) and stained with Coomassie Blue (Bio-Rad, Cat. No. 1610786). Presence of protein was confirmed using 10–180 kDa Prestained Protein Ladder (Fisher Scientific, Cat. No. 26616).

Purification of HLA-DQA1*01:01/DQB1*05:01 (DQ0101), HLA-DQA1*01:04/DQB1*05:03 (DQ0104), HLA-DQA1*01:05/DQB1*05:01 (DQ0105) and HLA-DRA1*01:01/DRB1*10:01 (DR10) was repeated in 5 l, as previously described.[45] Protein concentration was measured using a NanoDrop A280 and proteins were purified further by injection into a Superdex® 200 Increase 10/300 GL (GE Healthcare, Cat. No. GE17-5174-01) and Akta Pure fast protein liquid chromatography.

Identification of strong binder ligands specific to each HLA molecule

To identify possible reference ligands for HLA binding competition assays, we computationally predicted binding of different viral peptides to DQ0101, DQ0104, DQ0105 and DR10[46]: HIV Tat-specific factor 1, Plexin-C1, Epstein-Barr nuclear antigen 1 and 2, varicella-zoster virus and herpes simplex virus type 1. Seventeen 15-mer peptides were short-listed from this analysis as possible strong binders and synthesized biotin-conjugated at GenScript (NJ, USA) with >90% purity. Binding of these peptides to each HLA molecule was tested as described elsewhere.[45] In brief, CLIP peptides of purified HLA-monomers were removed using thrombin

cleavage (Millipore, Cat. No. 69671). In each well of a 96-well plate (Bio-Rad, Cat. No. MLP9601), 25 nM HLA-monomer was incubated with 10 μM biotin-conjugated ligand and 1× protease inhibitor (Sigma Aldrich, Cat. No. P8849), and the final reaction volume was increased to 30 μl using reaction buffer [100 mM acetate, pH 4.6, 150 mM NaCl, 1% bovine serum albumin (BSA) and 0.5% Nonidet P-40]. All reactions were tested both with and without the addition of 25 nM HLA-DM, and all reactions were tested at least in duplicate. Controls were run for each plate by substituting biotin-conjugated ligands for dimethyl sulphoxide (DMSO). Plates were sealed and incubated for 3 days at 37°C. The reaction was neutralized with 60 μl neutralization buffer (100 mM Tris-HCl, pH 8.6, 150 mM NaCl, 1% BSA, 0.5% Nonidet P-40 and 0.1% NaN_3) and transferred to a plate coated with monoclonal anti-DQ (Biotium, Cat. No. BNUM0200-50) or anti-DR antibody (BioLegend, Cat. No. 327002). Plates were incubated at room temperature for 1 h, washed five times with 300 μl 1× PBS supplemented with 0.05% Tween-20 (pH 7.4) and subsequently incubated for 1 h with 100 μl europium-labelled streptavidin (Cat. No. 1244-360, PerkinElmer) at a 1:1000 dilution in PBS with 1% BSA (pH 7.4). Plates were washed as described above, 100 μl enhancement solution (Cat. No. 1244-105, PerkinElmer) were added to each well and plates were placed on a shaker for 5 min. DELFIA® time-resolved fluorescence (TRF) intensity was detected using a Tecan Infinite® M1000 system. Following repetition of candidate binders using the above protocol in titrations of 100, 10 and 1 μM, KNIYIYLTAGKEVRR (bio-PLXC1, derived from Plexin C1) was confirmed as a strong-binding ligand to DQ0101, DQ0104 and DQ0105, and EDEIRGYKLHVEVAK (bio-HTSF1, derived from HIV Tat-specific factor 1) as a strong-binding ligand to DR10.

Competition binding assay

Fifteen-mer peptides with an 11-amino acid overlap covering the full length of IgLON5 and selected PTMs predicted using MusiteDeep,[47] NetPhos3.1,[48] NetNGlyc1.0[49] and mass spectrometry data from IgLON family members[50] (Fig. 3A and Supplementary Table 3) were synthesized with >90% purity at GenScript and dissolved in DMSO at a stock concentration of 10 mM. Competition binding assays were conducted using the same plate-binding assay used for the identification of strong binders. Specifically, each reaction contained 25 nM of thrombin-cleaved HLA-monomer, 400 μM of IgLON5 peptide and 10 μM of bio-PLXC1 or bio-HTSF1 (Fig. 3B and C) for DQ0101/DQ0104/DQ0105 and DR10 containing reactions, respectively. All reactions were tested both with and without the addition of 25 nM HLA-DM and in duplicate. Controls were run for each plate by substituting both IgLON5 and biotin-conjugated peptides for DMSO (negative control) or just IgLON5 peptides for DMSO (positive control). Peptides with Eu TRF intensity between 25% and 50% of that of bio-PLXC1/HTSF1 alone were considered weak binders, whereas any with intensity <25% were considered strong binders. Candidate binders were further tested in titration at competitor-to-peptide ratios of 1:40, 1:100 and 1:200, using 40, 100 and 200 μM of IgLON5 peptide and 1 μM of bio-PLXC1 or bio-HTSF1, for DQ0101/DQ0104/DQ0105 and DR10 containing reactions, respectively (Fig. 3D and E and Supplementary Fig. 7B and C).

Biotinylation of HLA-DQA1*01:05-DQB1*05:01 (DQ0105), peptide exchange and spheromer assembly

DQ0105 monomer was biotinylated (bio-DQ0105) using a BirA biotin-protein ligase standard reaction kit (Avidity, Cat. No. BirA500) and extra free biotin removed by injection into a Superdex® 200 Increase 10/300 GL (GE Healthcare, Cat. No. GE17-5174-01). Bio-DQ0105 was next transferred to a plate coated with monoclonal anti-DQ antibody (Biotium, Cat. No. BNUM0200-50), incubated for 1 h at room temperature and processed as described for the identification of strong binders. Biotinylation efficiency of the monomer was determined by detecting TRF intensity using a Tecan Infinite® M1000 system. Following this, bio-DQ0105 was cleaved and peptides exchanged as previously described[45] with ^{125}VYLIVHVPARIVDIS^{139} (bio-DQ0105/IgLON5). HLA-DM was removed and 5 μl of bio-DQ0105/IgLON5 (10 μM) incubated with 9.47 μl phycoerythrin-labelled streptavidin (2.78 μM, BioLegend, Cat. No. 405203) and 64.6 μl PBS (pH 7.4) for 30 min at room temperature. Uncleaved, unloaded bio-DQ0105 (bio-DQ0105/CLIP) (2.64 μM) was also incubated with 0.75 μl A488-labelled streptavidin (33.3 μM, BioLegend, Cat. No. 405235) and 59.3 μl PBS (pH 7.4) for 30 min at room temperature. The spheromers assembled with bio-DQ0105/CLIP monomers were used as a control for non-specific staining. Spheromer scaffold (0.9 μl, 471 μM)[51] and PBS (20 μl, pH 7.4) were added to each reaction, and following brief vortexing, incubated at room temperature for 30 min in the dark on a shaking incubator (Fig. 4A).

Peripheral blood mononuclear cells and sequencing of anti-IgLON5 antigen-specific CD4$^+$ T cells

Frozen peripheral blood mononuclear cells (PBMCs) were available from two patients with anti-IgLON5 disease carrying HLA-DQA1*01:05-DQB1*05:01 and from one HLA-matched control. Cells were thawed, counted and washed twice before settling in complete medium (RPMI 1640; Sigma Aldrich, Cat. No. 61770-036) supplemented with 10% heat-inactivated FBS (Gibco, Cat. No. 26140079) and 1× penicillin-streptomycin (Gibco, Cat. No. 15140122) and filtered through a 0.2 μm polyethersulphone (PES) membrane (Nalgene, Cat. No. 566-0020) at a concentration of 700 000 cells/300 μl/well in a 96-well flat bottom microplate (Thermo Fisher Scientific, Cat. No. 167008). Each well was stimulated with 1.875 μl of IgLON5-^{125}VYLIVHVPARIVDIS^{139} (1 mM) and incubated in a tissue culture incubator at 37°C, 5% CO_2 for 10 days. Medium was changed every 2–3 days and cells stimulated with IL-2 on Day 8. On Day 10, cells were washed and resuspended in 200 μl fluorescence-activated cell sorting (FACS) buffer (1× PBS, pH 7.4; Gibco, Cat. No. 10010023) supplemented with 2 mM EDTA (Sigma, Cat. No. E4884-500G) and 0.5% BSA (Sigma, Cat. No. A7888-50G), filtered through a 0.2 μm PES membrane (Nalgene, Cat. No. 566-0020). Cells were stained with 25 μl of each bio-DQ0105/IgLON5 and bio-DQ0105/CLIP spheromer and incubated at 37°C, 5% CO_2 for 90 min with gentle vortexing every 20 min. Cells were further stained with anti-CD3 (BioLegend, Cat. No. 317343), anti-CD4 (BioLegend, Cat. No. 300557), anti-CD8 (BioLegend, Cat. No. 301014) and Aqua live/dead stain (Invitrogen, Cat. No. L34965) prior to analysis with FACS. CD4$^+$/bio-DQ0105/IgLON5$^+$ cells were sorted into 96-well plates filled with capture buffer (Takara, Cat. No. 634439) and processed for single-cell sequencing and T-cell receptor sequencing as previously described.[45] Single-cell data were analysed using Scanpy.[52]

Standard protocol approvals, registrations and patient consents

This study was reviewed and approved by the Stanford University Institutional Review Board (Protocol No. 65073) as well as by local

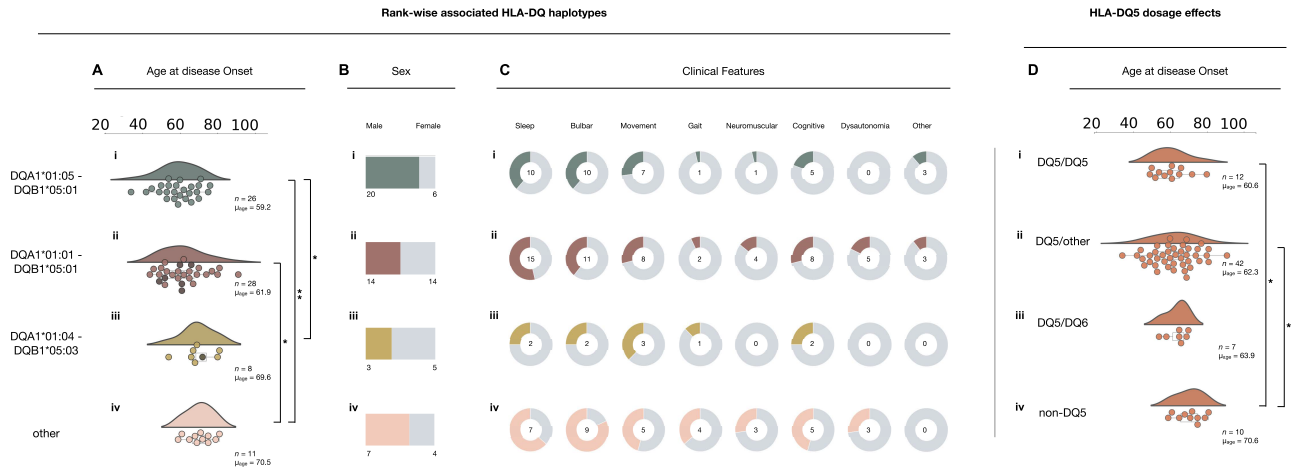

Figure 2 Delayed age of onset correlates with ranked HLA-risk and *HLA-DQ5* dosage. (**A**) Age at disease onset, (**B**) sex demographics and (**C**) major clinical features reported are shown for cases carrying (**i**) *HLA-DQA1*01:05-DQB1*05:01*, (**ii**) *HLA-DQA1*01:01-DQB1*05:01*, (**iii**) *HLA-DQA1*01:04-DQB1*05:03* or (**iv**) none of the aforementioned haplotypes. In **A**, coloured, filled circles indicate individual cases, whereas black filled markers denote homozygous carriers of the given haplotypes (Supplementary Table 2). In **C**, the numbers in the centres of the pie charts indicate the total numbers of cases reporting the given clinical feature. (**D**) Age at disease onset is shown for carriers (**i**) homozygous for *HLA-DQ5*, (**ii**) heterozygous for *HLA-DQ5* without *HLA-DQ6*, (**iii**) heterozygous for *HLA-DQ5*:~ with *HLA-DQ6*:~ and (**iv**) not carrying *HLA-DQ5*:~. For **D**(**i**), age range = 49–80 years ($\tilde{x}$ = 60.5 years); **D**(**ii**), age range = 34–91 years ($\tilde{x}$ = 62.0 years); **D**(**iii**), age range = 54–70 years ($\tilde{x}$ = 65.0 years); **D**(**iv**), age range = 59–81 years ($\tilde{x}$ = 71.5 years). *n* = total number of cases, μ_{age} = mean age, $\tilde{x}$ = median age, **P* < 0.05, ***P* < 0.01.

ethics committees of collaborating institutions. Written informed consent was obtained from all patients for the storage and use of biological samples and clinical information for research purposes.

Results

A primary association with HLA-DQ rather than HLA-DR in anti-IgLON5 disease

The intent of this study was to refine and extend prior HLA association studies in anti-IgLON5 disease. To do so, genome-wide SNP typing was conducted in 75/87 patients with the disease (Table 1, Supplementary Figs 1 and 2 and Supplementary Table 1), the largest sample ever studied. This was used to match cases to 232 controls by ethnicity using PCA (Fig. 1A) and to impute HLA. Any questionable samples and a random collection of samples were HLA-sequenced for verification.

Following HLA imputation and typing (Supplementary Figs 1 and 3), HLA association analysis revealed strong dominant associations with *HLA-DQB1*05:01* (frequency = 0.747, 56/75 patients), *HLA-DRB1*10:01* (frequency = 0.440, 33/75 patients) and *HLA-DQA1*01:05* (frequency = 0.413, 31/75 patients) in patients versus controls [Fig. 1B(i) and Table 2]. As shown in previous studies,[1,2,16] *HLA-DRB1*10:01* and *HLA-DQB1*05:01* showed the strongest association in terms of significance. Importantly, however, *HLA-DRB1*10:01*, *HLA-DQA1*01:05* and *HLA-DQB1*05:01* are in strong linkage disequilibrium (LD), forming a conserved haplotype[53] (Fig. 1C and Supplementary Fig. 4). As such, association is with the entire haplotype, and although risk is higher with *HLA-DRB1*10:01* and *HLA-DQA1*01:05*, *HLA-DQB1*05:01* is also present in other haplotypes and was more frequently associated with the disease, most notably in the context of *HLA-DRB1*01~DQA1*01:01~DQB1*05:01* haplotypes (Supplementary Fig. 4A).

Illustrating this, after excluding all carriers of *HLA-DRB1*10:01~DQB1*05:01* (33 cases and 6 controls), strong signals were still observed with *HLA-DQB1*05:01* (frequency = 0.548, 23/42 patients), followed by *HLA-DQA1*01:01* (frequency = 0.548, 23/42 patients) and *HLA-DRB1*01:01* (frequency = 0.452, 19/42 patients) [Fig. 1B(ii) and Table 2]. Once again, these alleles formed a common conserved haplotype (Fig. 1C and Supplementary Fig. 4), with only one subject carrying the *HLA-DRB1*01:02~DQA1*01:01~DQB1*05:01* haplotype. Given the remaining 19 patients did not carry either *HLA-DRB1*10:01~DQA1*01:05-DQB1*05:01* or *HLA-DRB1*01~DQA1*01:01~HLA-DQB1*05:01*, we further conditioned the analysis by removing carriers of *HLA-DRB1*01:01/*01:02* alleles as well, which thus removed any carriers of *HLA-DQA1*01:01~DQA1*05:01*. This identified a remaining association with *HLA-DQB1*05:03* (frequency = 0.368, 7/19 patients), *HLA-DQA1*01:04* (frequency = 0.368, 7/19 patients), *HLA-DRB1*14:54* (frequency = 0.211, 4/19 patients) and *HLA-DRB1*14:01* (frequency = 0.105, 2/19 patients) [Fig. 1C(iii) and Table 2]. Further conditioning with removal of *HLA-DQA1*01:04~DQB1*05:03* patients did not reveal additional significance [Fig. 1C(iv)].

Using genome-wide data, the highest association was with rs77456373 [minor allele frequency (MAF) = 0.32, OR = 4.09, $P = 1.26 \times 10^{-8}$, near *HLA-DQA1*], rs73729117 (MAF = 0.27, OR = 3.98, $P = 1.07 \times 10^{-8}$, near *HLA-DRB1*) and rs9271510 (MAF = 0.36, OR = 3.64, $P = 1.63 \times 10^{-8}$, near *HLA-DQA1*), all in tight LD ($r^2 > 0.8$) (Supplementary Fig. 2A). FINEMAP revealed two possible causal variants: rs17843573 with a probability of 0.99 (MAF = 0.40, r^2 = 0.56 with rs77456373) and rs9273329 with a probability of 0.96 (MAF = 0.43, r^2 = 0.64 with rs77456373). To confirm that these signals on chromosome 6 were secondary to the HLA association itself, we conditioned the GWAS association plot with rs73729117 (top SNP) (Supplementary Fig. 2B), rs17845573 (top FINEMAP SNP) (Supplementary Fig. 2C) and both (rs73729117 and rs17845573) (Supplementary Fig. 2D), showing that in all cases a residual effect above 10^{-5} remained in the HLA region. Similarly, controlling for *HLA-DQB1*05:01* only (which did not account for the strong effect of *HLA-DQA1*01:05* in conjunction with it), did not abolish the signal (Supplementary Fig. 2E). Only when all HLA effects we identified, *HLA-DQA1*01:05*, *HLA-DQA1*01:01* and *HLA-DQA1*01:04*, were taken into account, did all association signal effects in the DR and DQ

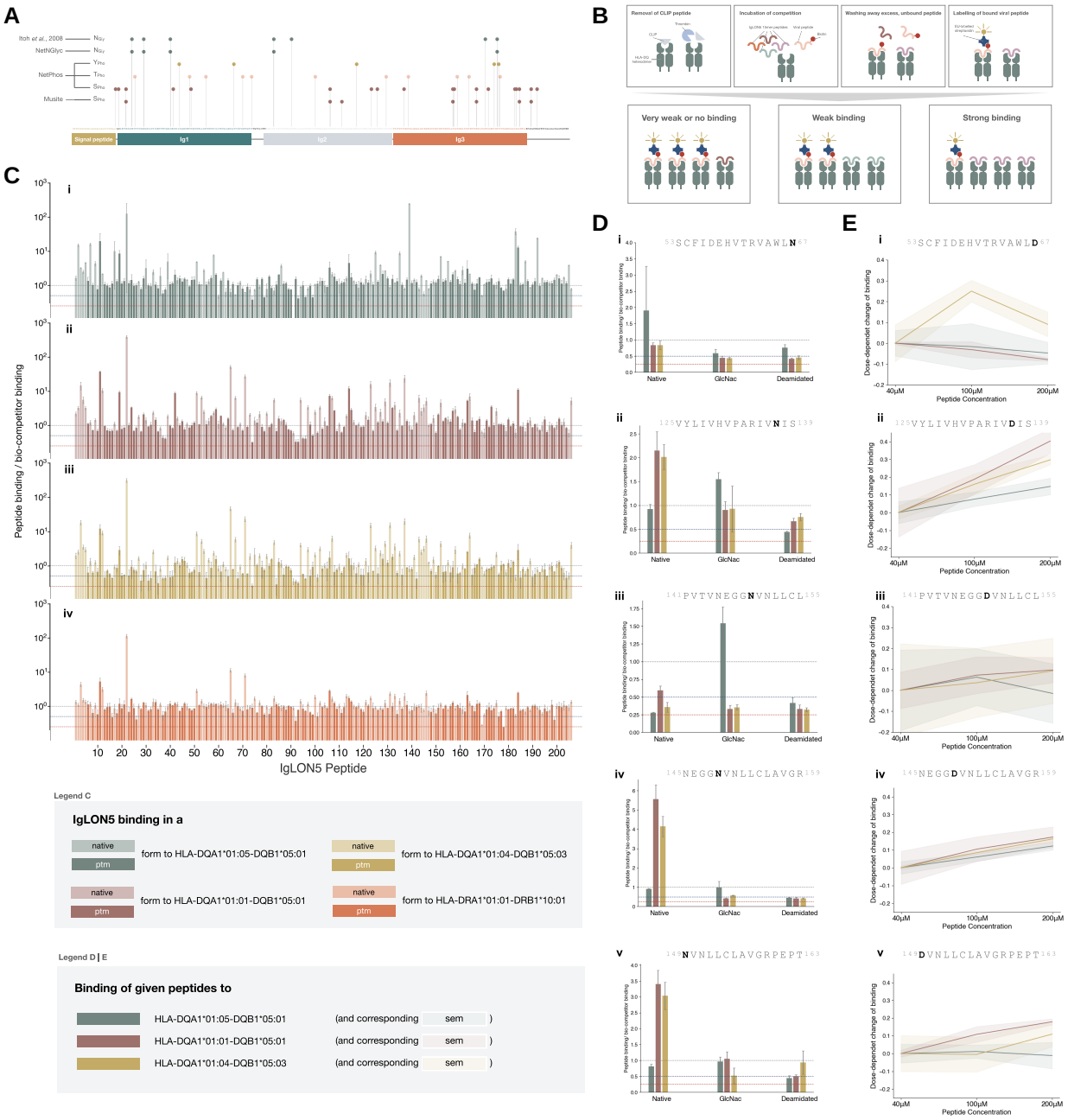

Figure 3 Risk-associated HLA-DQ5 molecules preferentially bind IgLON5 in a deamidated form. (**A**) The entire length and sequence of the IgLON5 peptide is shown, highlighting sites of post-translational modification (PTM) as predicted by MusiteDeep, NetPhos3.1, NetNGlyc1.0 and mass spectrometry data obtained from Itoh *et al.*[50] N_{glyc} = *N*-linked glycosylation, S_{phos} = serine phosphorylation, T_{phos} = threonine phosphorylation and Y_{phos} = tyrosine phosphorylation. (**B**) Schematic shows how peptide-HLA binding is determined using competition binding assay. (**C**) Results from competition binding assay are shown for (**i**) HLA-DQA1*01:05-DQB1*05:01, (**ii**) HLA-DQA1*01:01-DQB1*05:01, (**iii**) HLA-DQA1*01:04-DQB1*05:03 and (**iv**) HLA-DRA1*01:01-DRB1*10:01. Light bars show IgLON5 15mer peptides in native, and dark bars in PTM form (see legend at *bottom*). The *y*-axis (log scale) shows mean fluorescence intensity (mfi) of IgLON5 peptide together with biotinylated-competitor in competition, divided by the mfi of biotinylated-competitor alone. For **i–iii**, bio-PLXC1, and for **iv**, bio-HTSF1 was used as biotinylated-competitor. Along the *x*-axis, enumerated 15-mer IgLON5 peptides, sequentially encompassing the entire length of the IgLON5 protein, are shown (see Supplementary Table 3 for a full list of enumerated peptides). The dotted lines show the thresholds for weak (0.5) and strong (0.25) binders. (**D**) Binding of HLA-DQA1*01:05-DQB1*05:01 (green bars, *left* in each group), HLA-DQA1*01:01-DQB1*05:01 (purple bars, *middle* in each group) and HLA-DQA1*01:04-DQB1*05:03 (yellow bars, *right* in each group) to the five peptides (**i**) ^{53}SCFIDEHVTRVAWLN^{67}, (**ii**) ^{125}VYLIVHVPARIVNIS^{139}, (**iii**) ^{141}PVTVNEGGNVNLLCL^{155}, (**iv**) ^{145}NEGGNVNLLCLAVGR^{159} and (**v**) ^{149}NVNLLCLAVGRPEPT^{163} is shown, with asparagine residues (N) in bold in an unmodified ('native', *left*), glycosylated ('GLcNac', *middle*) or deamidated ('deamidated', *right*) form. Dotted lines as for **C**; *y*-axis is also as described for **C** but linear. (**E**) Dose-dependent change in binding of peptides described in **D**(**i–v**) when deamidated at bold N residues (i.e. mimicking aspartic acid, D). The *y*-axis shows dose-dependent change in binding as a ratio relative to baseline concentration used in **D** (40 µM of IgLON5 peptide), given the variation of IgLON5 peptide concentrations shown along the *x*-axis. Error bars in **C** and **D**, and shaded regions in **E**, represent the standard error of the mean (sem). All assays were repeated at least in duplicate.

Table 2 Conditioned HLA-association analysis

	Carriers			Alleles		
	Carrier frequency cases	Carrier frequency controls	P-value	Allele frequency cases	Allele frequency controls	P-value
No. of alleles excluded	**(*n* = 75)**	**(*n* = 232)**	–	**(*n* = 150)**	**(*n* = 464)**	–
DRB1*10:01	44% (33)	2.6% (6)	3.07×10^{-12}	22% (33)	1.3% (6)	3.07×10^{-12}
DQA1*01:05	41.3% (31)	2.2% (5)	2.63×10^{-11}	20.7% (31)	1.1% (5)	2.63×10^{-11}
DQB1*05:01	75% (56)	24.1% (56)	1.46×10^{-12}	41.3% (62)	13.8% (64)	2.69×10^{-10}
Exclude HLA-DRB1*10:01	**(*n* = 42)**	**(*n* = 226)**	–	**(*n* = 84)**	**(*n* = 452)**	–
DRB1*01:01	45.2% (19)	19% (43)	7.64×10^{-4}	27.4% (23)	10.2% (46)	1.77×10^{-4}
DRB1*01:02	11.9% (5)	4% (9)	2.20×10^{-2}	6% (5)	2% (9)	2.20×10^{-2}
DQA1*01:01	54.8% (23)	22.1% (50)	5.80×10^{-5}	33.3% (28)	12.2% (55)	1.38×10^{-5}
DQB1*05:01	54.8% (23)	22.1% (50)	5.80×10^{-5}	33.3% (28)	12.7% (57)	3.54×10^{-5}
Exclude HLA-DRB1*10:01, *01:01 and *01:02	**(*n* = 19)**	**(*n* = 176)**	–	**(*n* = 38)**	**(*n* = 352)**	–
DRB1*14:54	21.1% (4)	3.4% (6)	7.06×10^{-3}	13.2% (5)	1.7% (6)	4.70×10^{-3}
DRB1*14:01	10.5% (2)	1.1% (2)	2.90×10^{-2}	5.3% (2)	0.6% (2)	2.90×10^{-2}
DQA1*01:04	36.8% (7)	4.5% (8)	5.25×10^{-5}	21.1% (8)	2.3% (8)	6.39×10^{-5}
DQB1*05:03	36.8% (7)	4.5% (8)	5.25×10^{-5}	21.1% (8)	2.3% (8)	6.39×10^{-5}

regions disappear (Supplementary Fig. 2F and G). While confirming the identified HLA association, single SNP data should be treated with caution, subject to the small sample size.

Altogether, this analysis indicated a rank-wise association with *HLA-DRB1*10:01~DQA1*01:05~DQB1*05:01*, *DRB1*01~DQA1*01:01~DQB1*05:01* and *DRB1*14~DQA1*01:04~DQB1*05:03* haplotypes, in order of descending predisposing risk. Importantly, conservation of *DQA1*01-DQB1*05* (*HLA-DQ5*) with one to two amino acid differences across all three of these haplotypes (Supplementary Fig. 4B and C) indicated a primary role for HLA-DQ over HLA-DR.

HLA-DQ5 haplotypes associate with age at disease onset

Clinical data, together with (at least) 4-digit resolution HLA data for all *DR~DQ* loci, were available in 71 patients (Table 1, Supplementary Fig. 1 and Supplementary Table 1). Comparison of clinical characteristics identified a later mean age at disease onset, in line with carrier status for all three ranked *HLA-DQ5* haplotypes (Supplementary Table 2), which was significant for the two most dominant associations, *HLA-DQA1*01:05-DQB1*05:01* [Fig. 2A(i)] and *HLA-DQA1*01:01-DQB1*05:01* [Fig. 2A(ii)]. Specifically, subjects with *HLA-DQA1*01:05-DQB1*05:01*, *DQA1*01:01-DQB1*05:01* and *DQA1*01:04-DQB1*05:03* had a 11.3-, 8.6- and 0.9-years younger age of onset [Fig. 2A(i–iii)], compared with non-risk HLA haplotype carriers [Fig. 2A(iv)], respectively.

As previously reported,[16] we observed a higher proportion of male carriers with *HLA-DQA1*01:05-DQB1*05:01* (77% male versus 49% female, $P = 0.37$; Fig. 2B). Stratifying this analysis by gender showed a slightly older age at disease onset in females versus males [Supplementary Fig. 5A and B(i–iv)]; however, when controlling for gender as a covariate in the aforementioned analyses, the significance in the age shift (Fig. 1A) persisted [Supplementary Fig. 5C(i)]. We did not, however, confirm the presence of a sleep-dominant phenotype in *HLA-DRB1*10:01* carriers (43% versus 46% in non-*DRB1*10:01*, $P = 0.12$) as initially suggested.[16] Rather, stratifying by HLA-DQ5 revealed a more diverse clinical picture in non-*HLA-DQ5* versus *HLA-DQ5* carriers, although the numbers of non-DQ5 patients were too low to be conclusive for this subgroup (Fig. 2C). Moreover, there was no distinctive ethnicity associated with *HLA-DQ5* subtype, as determined by PCA (Supplementary Fig. 5D).

HLA-DQ5 dosage effects and allele competition stratify disease risk

Given that *HLA-DQA1*01*-encoded alpha chains can heterodimerize with either *HLA-DQB1*05*- or *06*-encoded beta chains, giving rise to DQ molecules with distinct binding profiles[54] (Supplementary Fig. 6), we investigated whether alterations in disease risk could occur in double-DQ1 heterozygotes, as reported for narcolepsy, where allele competition of other DQ1 molecules occurs with the DQ0602 heterodimer.[55] As predicted, we observed reduced frequency of trans-located *DQB1*06* (DQ6, non-IgLON5-susceptibility associated *DQ1* haplotypes) in patients versus controls (Table 3). Furthermore, age at disease onset was lowest in patients homozygous for *DQB1*05* (*DQ5/DQ5*), moderate for heterozygous carriers of *DQ5* with non-competing haplotypes (*DQ5*/other) and oldest in *DQ5/DQ6* heterozygotes [Fig. 2D and Supplementary Fig. 5A, B(v–viii) and C(ii)], suggesting that competition with non-susceptibility DQ1 alleles modulates age of onset. While onset occurred significantly earlier in *DQ5/DQ5* [Fig. 2D(i) and *DQ5*/other [Fig. 2D(ii)] subjects compared with non-*DQ5* carriers [Fig. 2D(iv)], this effect was abrogated when *DQ5* was inherited together with *DQ6* [Fig. 2D(iii)]. Altogether, these observations further support a functional role of *HLA-DQ5* in the development of anti-IgLON5 disease and suggest that rank-wise and dosage-dependent effects stratify disease risk.

Deamidation of N-glycosylation sites in the Ig2 domain primes IgLON5 peptide immunogenicity

To identify potential immunogenic IgLON5 peptides acting as T-cell auto-antigens, we derived 15-mer peptides (with 11-mer overlaps between peptides) encompassing the entire length of the IgLON5 protein (Fig. 3A and Supplementary Table 3) and screened these for binding (Fig. 3B) to all risk-associated *HLA-DQ5* molecules: HLA-DQA1*01:05-B1*05:01 [Fig. 3C(i)], DQA1*01:01-B1*05:01 [Fig. 3C(ii)] and DQA1*01:04-B1*05:03 [Fig. 3C(iii)], as well as to DRA1*01:01-DRB1*10:01 [Fig. 3C(iv)].

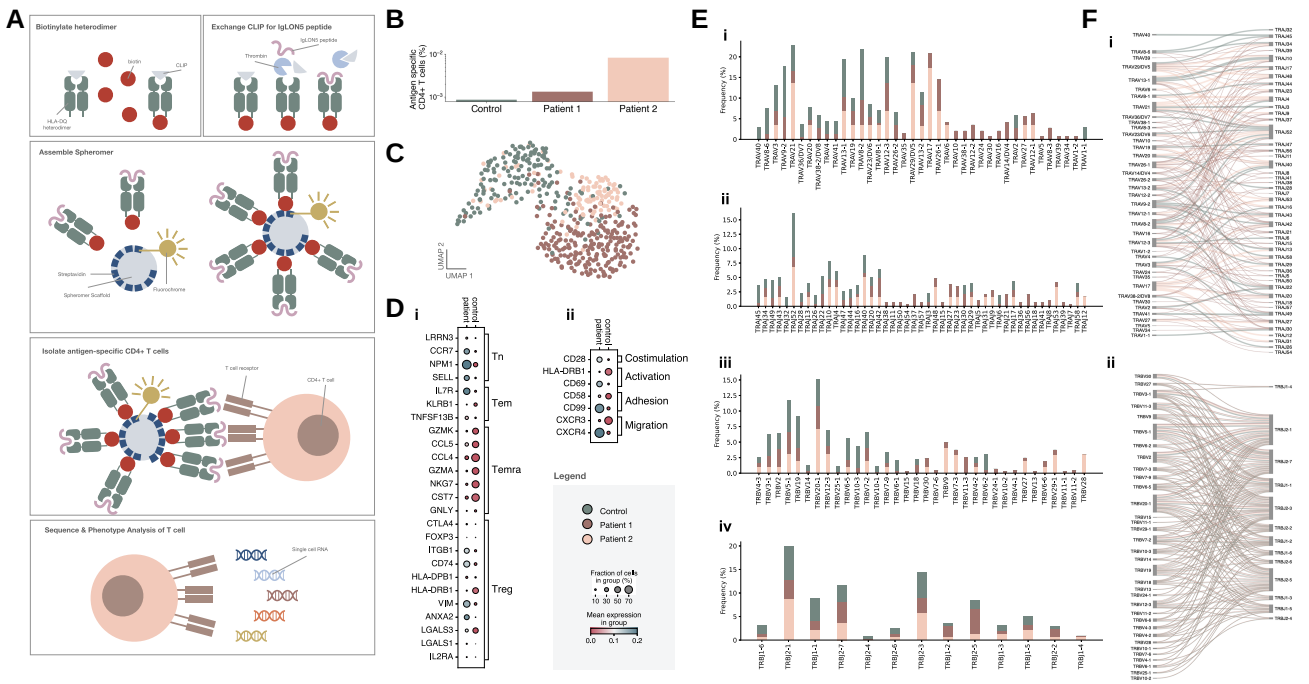

Figure 4 CD4⁺ T-cell reactivity and phenotypic profiling. (**A**) Schematic shows how peptide-HLA-spheromers are assembled and used to isolate antigen-specific CD4⁺ T cells. (**B**) Proportion of CD4+ T cells reactive to ^{125}VYLIVHVPARIVDIS^{139} in one control and two patients. (**C**) Neighbourhood clustering of isolated single cells by delineation into individuals [control (green), Patient 1 (purple), Patient 2 (pink)]. (**D**) T-cell markers. (**i**) Dot plot displays the expression levels of T-cell subset markers related to distinct transcriptional states in the control versus patient (Patients 1 and 2) group and (**ii**) related to distinct activation states. (**E**) T-cell receptor sequencing from antigen-specific cells isolated from control (green), Patient 1 (purple) and Patient 2 (pink) display the frequency of gene segments (**i**) TRAV, (**ii**) TRAJ, (**iii**) TRBV and (**iv**) TRBJ. (**F**) Pairings of (**i**) TRAV-TRAJ and (**ii**) TRBV TRBJ are shown. For **B**, **C**, **E** and **F**, see legend for colour coding and descriptions. T_{naive} = naive; T_{em} = effector; T_{emra} = highly effector; T_{reg} = regulatory.

In line with observations from other autoimmune diseases that show preferential immunogenic binding of peptides in PTM form,[30] we investigated possible modifications of IgLON5 (Fig. 3A). Computational predictions suggested that several serine, threonine and tyrosine residues could be phosphorylated,[47,48] and several asparagine residues *N*-linked glycosylated[49] (Fig. 3A). Notably, mass spectrometry confirmed several *N*-glycosylation sites in homologous IgLON peptides,[50] consistent with previous work.[56] Similarly, asparagine and glutamine can also be chemically deamidated as a result of protein ageing, which is a possibility, considering that the half-life of surface-expressed IgLON5 is over 3 days *in vitro* and could be higher in neurons.[57-60] We computationally predicted binding of these modified forms of IgLON5 to HLA molecules and subsequently narrowed down 124 15-mer peptides that we further tested using *in vitro* competition binding assay.

In general, we observed higher binding of peptides in their modified versus native forms (Fig. 3C and Supplementary Fig. 7A). We identified a handful of promising binders (e.g. IgLON5_91, IgLON5_178; Fig. 3C) that we titrated at different concentrations (Supplementary Fig. 7B and C). Higher binding at increasing concentrations suggests that the candidate peptide has a sound affinity for the HLA molecule, indicating their potential as strong binders with favourable HLA molecule interactions and immunogenicity profiles.

Notably, we found several peptides that bound disease-associated *HLA-DQ5* monomers preferably when asparagine residues (N) N_{67} [Fig. 3D(i) and E(i)], N_{137} [Fig. 3D(ii) and E(ii)] or N_{149} [Fig. 3D(iii–v) and E(iii–v)] were substituted for aspartic acid (D). N to D substitution mimics deamidation of key *N*-glycosylation sites,[61] a PTM that is a known contributor to reducing self-tolerance and priming peptides for autoimmune T-cell recognition.[62,63] While HLA binding affinity of several initial candidate peptides was not confirmed by further titration experiments, such as IgLON5_91 [Fig. 3E(i, iii and v) and Supplementary Fig. 7], the two deamidated peptides ^{125}VYLIVHVPARIV**N**IS^{139} $N > D_{137}$ [Fig. 3E(ii)] and ^{145}NEGG**N**VNLLCLAVGR^{159} $N > D_{149}$ [Fig. 3E(iv)] showed a dose-dependent increase in binding, whereas their native or glycosylated forms did not (Supplementary Fig. 7C), thus confirming their strong HLA affinity and relevance as strong binders.

Moreover, comparison of the binding motifs of risk-associated HLA-DQ5 molecules showed that all three HLA-DQs bind D with high-affinity in pocket six of the 9-mer binding core (Supplementary Fig. 4B and C), thus further substantiating that deamidation may be key to making these peptides immunogenic.

Taken together, these results suggest that deamidation of specific asparagine sites within the IgLON5-Ig2 domain might prime specific IgLON5 peptides for HLA class II presentation through risk-associated HLA-DQ5 molecules.

Increased CD4⁺ T cell reactivity to a deamidated IgLON5-Ig2-derived peptide

To test whether deamidation may be a key modification to evoke a functional autoimmune response, we stimulated PBMCs of two *HLA-DQA1*01:05-DQB1*05:01*-carrying patients and one HLA-matched control with an Ig2-derived 15-mer peptide, ^{125}VYLIVHVPARIVDIS^{139}, mimicking deamidation at N_{137} for 10 days, prior to isolating antigen-specific CD4⁺ T cells using spheromer[51] (Fig. 4A). Notably, the low frequency of *HLA-DQA1* 01:05-DQB1*05:01* in the general population (~2%) substantially challenged the screening for suitable HLA-matched control

Table 3 Frequency of HLA-DQ5 and HLA-DQ6 haplotypes

	Homozygous				Heterozygous			
	Cases ($n = 75$)	Controls ($n = 232$)	OR	$\chi 2$	Cases ($n = 75$)	Controls ($n = 232$)	OR	$\chi 2$
HLA-DQ5 haplotypes								
DQA1*01:-DQB1*05:	13.3% (10)	3.9% (9)	16.87	5.04×10^{-9}	72% (54)	24.1% (56)	14.64	8.89×10^{-17}
DQA1*01:05-DQB1*05:01	0% (0)	0% (0)	–	–	41.3% (31)	2.2% (5)	31.99	3.22×10^{-19}
DQA1*01:01-DQB1*05:01	6.7% (5)	2.2% (5)	3.65	8.52×10^{-2}	28% (21)	20.7% (48)	1.60	1.70×10^{-1}
DQA1*01:04-DQB1*05:03	1.3% (1)	0% (0)	–	–	9.3% (7)	3.9% (9)	2.59	1.15×10^{-1}
DQA1*01:02-DQB1*05:02	–	–	–	–	4% (3)	0.4% (1)	9.63	7.45×10^{-2}
HLA-DQ6 haplotypes								
DQA1*01:-DQB1*06:	0% (0)	0.039 (9)	–	–	13.3% (10)	36.2% (84)	0.25	1.57×10^{-4}
DQA1*01:03-DQB1*06:03	0% (0)	0% (0)	–	–	6.7% (5)	11.2% (26)	0.57	3.61×10^{-1}
DQA1*01:02-DQB1*06:02	0% (0)	0.009 (2)	–	–	4% (3)	15.1% (35)	0.23	1.86×10^{-2}
DQA1*01:02-DQB1*06:09	0% (0)	0% (0)	–	–	1.3% (1)	2.2% (5)	0.61	9.99×10^{-1}
DQA1*01:02-DQB1*06:04	0% (0)	0.004 (1)	–	–	1.3% (1)	7.8% (18)	0.16	8.21×10^{-2}

OR = odds ratio.

PBMCs. Both patients showed elevated $CD4^+$ T-cell reactivity compared with the control, although this was more pronounced in Patient 2 (Fig. 4B). Antigen-specific $CD4^+$ T cells were sorted and sequenced to investigate cellular phenotypes. While there was some admixture, patient cells formed a distinct cluster relative to control cells (Fig. 4C), suggesting similarities in affinities and possible clonality. Delineation into distinct T-cell transcriptional states, namely naive (T_{naive}), effector (T_{em}), highly effector (T_{emra}) and regulatory (T_{reg}) T-cell subsets [Fig. 4D(i)], underscored the expression of T_{emra} markers in the control versus patient population, while elevated activation and proliferation [Fig. 4D(ii)] in the latter population further supported the suggestion that antigen-specific T cells are more highly differentiated in patients. Furthermore, T-cell receptors (TCR) were sequenced and *TRAV*, *TRAJ*, *TRBV* and *TRBJ* gene segments studied (Fig. 4E); these make up the TCR alpha and beta chains and play a crucial role in the diversity and specificity of HLA-peptide-TCR interactions. In doing so, we identified several segments, especially in the TCR alpha chain, that were unique to patients [Fig. 4E(i and ii)]. Looking at pairings of *TRAV*, *TRAJ*, *TRBV* and *TRBJ* (Fig. 3F), we corroborated the finding of individual pairings in patients; however, several combinations were also found to be unique to the control.

Taken together, these preliminary findings suggested that reactivity against deamidated Ig2-derived IgLON5 may be elevated in anti-IgLON5 disease subjects and that unique TCR signatures associated with a more effector T-cell phenotype can be found.

Discussion

This study is the largest reported HLA-association analysis in anti-IgLON5 disease. Notably, it benefits from the inclusion of patients from multiple different ethnicities and countries and rigorous matching of controls by PCA.[39] In this work, we were able to confirm and refine the association of anti-IgLON5 disease with *HLA-DQ* over *HLA-DR*.[2,16] Interestingly, *HLA-DQ5*-dosage effects modulated both disease predisposition (haplotype carrier frequency differences) and age at disease onset, with a protective effect of *HLA-DQ6*, possibly through allele competition with *HLA-DQ5*. Future studies investigating the effects of these combinations on HLA-DQ5 expression and how trans-dimerization may affect HLA-peptide binding[64,65] will be needed to further substantiate these observations.

A ranked association with three *HLA-DQ5* haplotypes, *HLA-DQA1*01:05-05:01*, *HLA-DQA1*01:01-05:01* and *HLA-DQA1*01:04-05:03*, in order of descending risk was found in 85% (74/87) of all patients and further reflected in a delayed age at disease onset. Altogether, this strongly supports *HLA-DQ*, and not *HLA-DR*, as the actual determinant for disease risk. Disease risk in the remaining patients could not be explained by HLA; however, the fact that non-*HLA-DQ5* carriers have a significantly later age at disease onset suggests that there might be a distinct trigger. While a previous report suggested more dominant presentation of sleep or bulbar symptoms in *HLA-DRB1*10:01*-carriers,[16] we were not able to confirm this observation, nor decipher any other significant associations between HLA-haplotype and major clinical phenotypes. Interestingly, a retrospective analysis of clinical, polysomnographic and HLA data[66] showed a high prevalence of *HLA-DQB1*05:01* in different types of NREM parasomnias, thus suggesting that stratification of sleep phenotypes may occur at the level of *HLA-DQB1*05*, as opposed to distinct *HLA-DRB1~DQA1~DQB1* haplotypes. However, a recent report[67] showed that a progressive supranuclear palsy-like phenotype was underrepresented in *HLA-DRB1*10:01*-carriers, while carrier status did not affect the development of movement disorders more generally, suggesting that stratification of clinical phenotypes by HLA-carrier status may only occur at the level of specific clinical features. Future clinical reports should thus focus on a more fine-grained analysis of HLA association with detailed clinical phenotypes.

We did not observe that native IgLON5 peptides strongly bound HLA-DQ5. Rather, in line with observations from other autoimmune diseases such as type-1 diabetes mellitus or rheumatoid arthritis,[30] HLA-DQ5 was found to bind PTM IgLON5 peptides containing aspartic acid residues in several positions. In line with this observation, it is worth noting that HLA-DQA1*01:05/DQB1*05:01, HLA-DQA1*01:01/DQB1*05:01 and HLA-DQA1*01:04/DB1*05:03 all bind D in pocket six with high affinity, although less pre-eminently so for HLA-DQA1*01:04/DQB1*05:03 (Supplementary Fig. 4B). Deamidation that substitutes N for D can occur as proteins age and are targeted for degradation, and it has thus been suggested that this modification may serve as an age-dependent molecular clock,[57,61] an intriguing concept considering the late age of onset of the disease and slow turnover of the IgLON5 protein as has been shown by Heo *et al.*[59] (refer to Supplementary Table 2 in the aforementioned work). While deamidation of asparagine was previously shown to alter both HLA class II antigen presentation,[63] as well as

T-cell recognition,[68] the physiological relevance of this modification in anti-IgLON5 disease remains enigmatic. Our hypothesis is that deamidations occur *in vivo* as the result of simple chemical deamidation,[61] enzymatic deamidation or following de-glycosylation of *N*-linked glycopeptides at the corresponding residues,[69] although this latter mechanism was primarily shown for HLA-class I presentation of intracellularly processed peptides.[70] Notably, deficiency of the enzyme NGLY1, which catalyses the removal of *N*-linked glycans and plays a key role in endoplasmic reticulum-associated degradation, was recently discovered to be the cause of a severe, multisymptomatic disorder that also involves a complex movement disorder,[71,72] while abnormalities in the NGLY1–NRF1 pathway have been associated with immune dysregulation.[73] Whether abnormalities in enzymatic *N*-deglycosylation could play a role in this process may therefore also be considered. Overall, a considerable shortcoming in the field of anti-IgLON5 disease research is the concurrent lack of availability of mass spectrometric or comparable proteomic data needed to confirm PTM changes speculated to occur in this condition beyond computational predictions. The significance of the PTM modifications suggested here, and their relevance and importance in triggering the disease, therefore need to be confirmed *in vivo*.[74]

Of note, it has previously been suggested that the IgLON5-derived peptides ^{10}LRLLAAAAL^{19} and ^{127}IVHVPARIV^{136} constitute potential causative immunogenic cores, due to their high computationally predicted binding affinity to HLA-DRA1*01:01-DRB1*10:01 and HLA-DRA1*01:01-DRB1*01:01.[16] Testing these peptides *in vitro*, however, we could not confirm binding of either peptide to HLA-DRA1*01:01-DRB1*10:01. Altogether, the fact that HLA-DRA1*01:01-DRB1*10:01 neither accounts for genetic risk in most patients nor shows binding of the proposed peptides, does not favour a role for HLA-DR in the disease. Furthermore, these results highlight the limitations of *in silico* predictions[75] and stress the importance of *in vitro* binding assays to substantiate any autoimmune HLA-peptide interactions.

The deamidated peptide we identified as HLA-DQ5-binder lies within the Ig2 domain of IgLON5. Interestingly, the Ig2 domain was previously shown to be the key target site of patient autoantibody recognition[56] and treatment with bacterial-derived PNGase F (*N*-glycosidase F, an endoglycosidic enzyme that deamidates *N*-glycosylated residues to aspartic acid through removal of oligosaccharides from glycoproteins) maintained autoantibody binding to IgLON5-expressing cells.[76] The binding of deamidated peptides to the risk-associated HLA-molecules we have shown here therefore corresponds with previously reported autoantibody target sites both in terms of location along the IgLON5 protein and the state of PTM. This suggests that B-cell and T-cell epitopes involved in the diseases may overlap or be in close proximity as is sometimes observed following epitope spreading.[77] T–B-cell interactions are a critical component of the pathophysiological trajectory in most autoimmune diseases[21,78] and the study at hand lays an important foundation for further investigation of this important interaction (Supplementary Fig. 8).

In the current study, we showed elevated T-cell reactivity against a single modified epitope, ^{125}VYLIVHVPARIVDIS^{139} in two patients, compared with a single HLA-matched control. We used spheromers, state-of-the-art multimers that allow more efficient T-cell staining and improved TCR-binding properties,[51] enabling the detection of low-affinity T cells that may be more disease relevant in autoimmunity.[79,80] While the T-cell data we present suggest functional relevance of ^{125}VYLIVHVPARIVDIS^{139} in shaping an early autoimmune response in anti-IgLON5 disease driven by T cells in a late effectorness state,[81] these data should be considered preliminary, subject to the small sample size. Randomized screening for the identification of matched HLA-control PBMCs proved challenging in the concurrent study, given the low frequency (~2%) of *HLA-DQA1*01:05-DQB1*05:01* in the general population. Future studies testing additional subjects and epitopes will be needed to confirm the relevance of ^{125}VYLIVHVPARIVDIS^{139} and other epitopes in shaping anti-IgLON5 autoimmunity, as well as to define phenotypic signatures of disease-relevant, antigen-specific T cells. Similarly, the TCR sequencing data we have shown here is suggestive of unique TCRs in patients versus controls and motivates further assessment of TCR diversity, both in more patient and control subjects but also using different autoantigen candidate peptides and carriers of different *HLA-DQ5* subtypes. Whether reactivity against the same epitope is shared across carriers of distinct HLA-DQ5 molecules, as suggested by the shared HLA-peptide binding properties shown in our current study, will require further examination. We hypothesize that future studies focusing on T-cell reactivity against multiple IgLON5-derived epitopes in distinct HLA-DQ5 carriers may explain the ranked-*HLA-DQ5* disease risk, which the current study promotes on the basis of genetic, demographic and molecular evidence.

Taken together, this study has important pathophysiological and clinical implications for our understanding of anti-IgLON5 disease. First, it shows for the first time that anti-IgLON5 disease is primarily *HLA-DQ* associated, and that T-cell autoimmunity directed towards deamidated IgLON5 sequences presented by these molecules may be involved. Second, a delay in the age at disease onset between different *HLA-DQ5* subtypes implies clinical differences secondary to peptide presentation by slightly different HLA-DQ heterodimers; thus, future studies should further investigate symptomatic and disease outcome distinctions between different *HLA-DQ5* subtypes. Future studies incorporating a larger number of patients, a difficult endeavour in a rare disease, will be needed to further elucidate the genetic risk of this condition also at a genome-wide level. Concurrent to that, investigations of immune cell reactivity and phenotypes will be required to elucidate key pathophysiological events, aimed at disentangling the intricate interplay of autoimmunity and neurodegeneration within, and beyond, this condition. Ultimately, this understanding will pave the way to developing more effective therapeutics (e.g. targeting autoantigen-specific CD4$^+$ T cells), promising to halt irreversible neurodegenerative mechanisms upstream in the pathology, thus instituting vital treatment strategies that currently remain amiss for this condition.

Data availability

Raw data are available on request to the corresponding author.

Acknowledgements

We thank Christopher Garcia (Stanford University) for providing insect cell lines, Gonzalo Montero-Martin and Marcelo Fernandez-Viña for HLA-validation typing, Daniel Fernandez for technical support during AKTA-FPLC and both the Stanford FACS and HIMC facilities for support with T cell isolation and sequencing, respectively. We also would like to thank all collaborators and doctors, who referred patients to this study, beyond those listed as co-authors: Olivier Flabeau (Bayonne, France), Eve Chanson (Clermont Ferrand, France), Mathilde Compoint (Dieppe, France), Tifanie Alberto (Lille, France), Julie Boucher (Lille, France), Isabelle

Francillard (Lorient, France), Emilien Bernard (Lyon, France), Virginie Desestret (Lyon, France), Philippe Damier (Nantes, France), Nicolas Capet (Nice, France), Caroline Giordana (Nice, France), Dimitri Renard (Nîmes, France), Aurélie Meneret (Paris, France), Foucaud Du Boisgueheneuc (Poitiers, France), Maximilien Moulin (Reims, France), Flora Delamaire (Rennes, France), Marie Rafiq (Toulouse, France), Gilles Ryckewaert (Valenciennes, France).

Funding

This study was primarily funded by a seed grant awarded by The Stanford Autoimmune & Allergy Supergroup (SAAS) to E.M. and National Institutes of Health grant NIH-5U01NS120885-02. S.M.Y. received funding from the Einstein Center for Neurosciences Berlin (Einstein Foundation Berlin) and the German-Academic Exchange Service (DAAD). The French collection of samples is developed within the BETPSY project, which is supported by a public grant overseen by the French National Research Agency (ANR), as part of the second 'Investissements d'Avenir' program (reference ANR-18-RHUS-0012) and J.H. is supported by the European Reference Networks, the Research and Innovative Technology Administration and LabEx CORTEX (ANR-11-LABX-0042). C.F. is supported by the Deutsche Forschungsgemeinschaft (DFG, German Research Foundation), grant numbers FI 2309/1-1 and FI 2309/2-1; and the Federal Ministry of Education and Research (Bundesministerium für Bildung und Forschung), grant number 01GM1908D (CONNECT-GENERATE). S.I. is supported by a senior clinical fellowship from the Medical Research Council (MR/V007173/1), Wellcome Trust Fellowship (104079/Z/14/Z), British Medical Association Research Grants- Vera Down grant (2013) and Margaret Temple (2017), Epilepsy Research UK (P1201), the US-UK Fulbright Commission (MS-Society research award) and by the National Institute for Health Research (NIHR) Oxford Biomedical Research Centre (BRC). For the purpose of Open Access, the author has applied a CC BY public copyright licence to any Author Accepted Manuscript (AAM) version arising from this submission. The views expressed are those of the author(s) and not necessarily those of the NHS, the NIHR or the Department of Health. L.S. is funded in part by Instituto de Salud Carlos III through the project FIS21/00165 (L.S., C.G.) (co-funded by the European Regional Development Fund 'Investing in your future'). We thank the European Joint Programme on Rare Diseases (EJPRD) for funding a Networking event (contract number 463001015) on IgLON5 disease from the European Union's Horizon 2020 research and innovation programme under the EJP RD COFUND-EJP N°825575. B.S. received funding through the Betty and David Koetser Foundation, Neuromuscular Research Association Basel. T.S. (22K07492) and A.K. (JP21K07457) received Grants-in-Aid for Scientific Research (C) from the Japan Society for the Promotion of Science. H.P. is supported by the German Research Foundation (DFG; grants FOR3004, PR1274/3-1, PR1274/5-1, and PR1274/9-1), Helmholtz Association (HIL-A03 BaoBab), and Bundesministerium für Bildung und Forschung (German Federal Ministry of Education and Research) (Connect-Generate 01GM1908D). A.M. is supported by National Institutes of Health (NIH): RO1NS126227, U01NS12090. J.D. is supported by Caixa Research Health 2022 (HR22-00221). This study was funded also in part by Instituto de Salud Carlos III (ISCIII)—Fondo de Investigaciones Sanitaria (FIS) through the project 'PI21/00165' (L.S. and C.G.) and the Networking Support Scheme funded from the European Union's Horizon 2020 research and innovation programme under the EJP RD COFUND-EJP No. 825575.

Competing interests

S.R.I. has received honoraria/research support from UCB, Immunovant, MedImmun, Roche, Janssen, Cerebral therapeutics, ADC therapeutics, Brain, CSL Behring and ONO Pharma; and receives licensed royalties on patent application WO/2010/046716 entitled 'Neurological Autoimmune Disorders'; and has filed two other patents entitled 'Diagnostic method and therapy' (WO2019 211633 and US-2021-0071249-A1; PCT application WO2021897 88A1) and 'Biomarkers' (PCT/GB2022/050614 and WO202189788A1). S.M. received speaker honoraria from Biogen, Sanofy and Novartis. C.J.H. has been serving as a consultant for Univar and has received honoraria for lecturing and travel expenses/speaking honoraria from Abbott and Alexion and research support from Abbott. A.M. patents issued for GFAP and MAP1B-IgGs and patents pending for PDE10A, Septins-5 and -7 and KLCHL11-IgGs, and has consulted for Janssen and Roche pharmaceuticals, without personal compensation. J.D. holds a patent for the use of IgLON5 antibody testing and both he and F.G. receive royalties from Euroimmun for the clinical use of this test. The other authors report no competing interests.

Supplementary material

Supplementary material is available at *Brain* online.

References

1. Sabater L, Gaig C, Gelpi E, et al. A novel non-rapid-eye movement and rapid-eye-movement parasomnia with sleep breathing disorder associated with antibodies to IgLON5: A case series, characterisation of the antigen, and post-mortem study. *Lancet Neurol*. 2014;13:575-586.
2. Grüter T, Möllers FE, Tietz A, et al. Clinical, serological and genetic predictors of response to immunotherapy in anti-IgLON5 disease. *Brain*. 2023;146:600-611.
3. Gelpi E, Höftberger R, Graus F, et al. Neuropathological criteria of anti-IgLON5-related tauopathy. *Acta Neuropathol*. 2016;132:531-543.
4. Berger-Sieczkowski E, Endmayr V, Haider C, et al. Analysis of inflammatory markers and tau deposits in an autopsy series of nine patients with anti-IgLON5 disease. *Acta Neuropathol*. 2023;146:631-645.
5. Schöberl F, Levin J, Remi J, et al. IgLON5: A case with predominant cerebellar tau deposits and leptomeningeal inflammation. *Neurology*. 2018;91:180-182.
6. Cagnin A, Mariotto S, Fiorini M, et al. Microglial and neuronal TDP-43 pathology in anti-IgLON5-related tauopathy. *J Alzheimers Dis*. 2017;59:13-20.
7. Erro ME, Sabater L, Martínez L, et al. Anti-IGLON5 disease: A new case without neuropathologic evidence of brainstem tauopathy. *Neurol Neuroimmunol Neuroinflamm*. 2020;7:e651.
8. Cabezudo-Garcia P, Mena-Vazquez N, Estivill Torrus G, Serrano-Castro P. Response to immunotherapy in anti-IgLON5 disease: A systematic review. *Acta Neurol Scand*. 2020;141:263-270.
9. Fearnley S, Raja R, Cloutier JF. Spatiotemporal expression of IgLON family members in the developing mouse nervous system. *Sci Rep*. 2021;11:19536.
10. Hashimoto T, Maekawa S, Miyata S. IgLON cell adhesion molecules regulate synaptogenesis in hippocampal neurons. *Cell Biochem Funct*. 2009;27:496-498.
11. Lim JH, Beg MMA, Ahmad K, et al. IgLON5 regulates the adhesion and differentiation of myoblasts. *Cells*. 2021;10:417.

12. Vanaveski T, Singh K, Narvik J, et al. Promoter-specific expression and genomic structure of IgLON family genes in mouse. *Front Neurosci*. 2017;11:38.
13. Landa J, Gaig C, Plaguma J, et al. Effects of IgLON5 antibodies on neuronal cytoskeleton: A link between autoimmunity and neurodegeneration. *Ann Neurol*. 2020;88:1023-1027.
14. Ryding M, Gamre M, Nissen MS, et al. Neurodegeneration induced by anti-IgLON5 antibodies studied in induced pluripotent stem cell-derived human neurons. *Cells*. 2021;10:837.
15. Ni Y, Feng Y, Shen D, et al. Anti-IgLON5 antibodies cause progressive behavioral and neuropathological changes in mice. *J Neuroinflammation*. 2022;19:140.
16. Gaig C, Ercilla G, Daura X, et al. HLA and microtubule-associated protein tau H1 haplotype associations in anti-IgLON5 disease. *Neurol Neuroimmunol Neuroinflamm*. 2019;6:e605.
17. Dahal-Koirala S, Ciacchi L, Petersen J, et al. Discriminative T-cell receptor recognition of highly homologous HLA-DQ2-bound gluten epitopes. *J Biol Chem*. 2019;294:941-952.
18. Lim JJ, Jones CM, Loh TJ, et al. The shared susceptibility epitope of HLA-DR4 binds citrullinated self-antigens and the TCR. *Sci Immunol*. 2021;6:eabe0896.
19. Luo G, Ambati A, Lin L, et al. Autoimmunity to hypocretin and molecular mimicry to flu in type 1 narcolepsy. *Proc Natl Acad Sci U S A*. 2018;115:E12323-E12332.
20. Binks S, Varley J, Lee W, et al. Distinct HLA associations of LGI1 and CASPR2-antibody diseases. *Brain*. 2018;141:2263-2271.
21. Lanzavecchia A. Antigen-specific interaction between T and B cells. *Nature*. 1985;314:537-539.
22. Klein J, Sato A. The HLA system. *N Engl J Med*. 2000;343:702-709.
23. Bjornevik K, Cortese M, Healy BC, et al. Longitudinal analysis reveals high prevalence of Epstein-Barr virus associated with multiple sclerosis. *Science*. 2022;375:296-301.
24. Steinman L, Patarca R, Haseltine W. Experimental encephalomyelitis at age 90, still relevant and elucidating how viruses trigger disease. *J Exp Med*. 2023;220:e20221322.
25. Han F, Lin L, Warby SC, et al. Narcolepsy onset is seasonal and increased following the 2009 H1N1 pandemic in China. *Ann Neurol*. 2011;70:410-417.
26. Partinen M, Saarenpää-Heikkilä O, Ilveskoski I, et al. Increased incidence and clinical picture of childhood narcolepsy following the 2009 H1N1 pandemic vaccination campaign in Finland. *PLoS One*. 2012;7:e33723.
27. Schellekens GA, de Jong BA, van den Hoogen FH, van de Putte LB, van Venrooij WJ. Citrulline is an essential constituent of antigenic determinants recognized by rheumatoid arthritis-specific autoantibodies. *J Clin Invest*. 1998;101:273-281.
28. Arribas-Layton D, Guyer P, Delong T, et al. Hybrid insulin peptides are recognized by human T cells in the context of DRB1*04:01. *Diabetes*. 2020;69:1492-1502.
29. Tran MT, Faridi P, Lim JJ, et al. T cell receptor recognition of hybrid insulin peptides bound to HLA-DQ8. *Nat Commun*. 2021;12:5110.
30. Raposo B, Merky P, Lundqvist C, et al. T cells specific for post-translational modifications escape intrathymic tolerance induction. *Nat Commun*. 2018;9:353.
31. Gaig C, Graus F, Compta Y, et al. Clinical manifestations of the anti-IgLON5 disease. *Neurology*. 2017;88:1736-1743.
32. Bonello M, Jacob A, Ellul MA, et al. IgLON5 disease responsive to immunotherapy. *Neurol Neuroimmunol Neuroinflamm*. 2017;4:e383.
33. Honorat JA, Komorowski L, Josephs KA, et al. IgLON5 antibody: Neurological accompaniments and outcomes in 20 patients. *Neurol Neuroimmunol Neuroinflamm*. 2017;4:e385.
34. Montagna M, Amir R, De Volder I, Lammens M, Huyskens J, Willekens B. IgLON5-associated encephalitis with atypical brain magnetic resonance imaging and cerebrospinal fluid changes. *Front Neurol*. 2018;9:329.
35. Fuseya K, Kimura A, Yoshikura N, Yamada M, Hayashi Y, Shimohata T. Corticobasal syndrome in a patient with anti-IgLON5 antibodies. *Mov Disord Clin Pract*. 2020;7:557-559.
36. Tagliapietra M, Frasson E, Cardellini D, et al. Hypothalamic-bulbar MRI hyperintensity in anti-IgLON5 disease with serum-restricted antibodies: A case report and systematic review of literature. *J Alzheimers Dis*. 2021;79:683-691.
37. Werner J, Jelcic I, Schwarz EI, et al. Anti-IgLON5 disease: A new bulbar-onset motor neuron mimic syndrome. *Neurol Neuroimmunol Neuroinflamm*. 2021;8:e962.
38. Purcell S, Neale B, Todd-Brown K, et al. PLINK: A tool set for whole-genome association and population-based linkage analyses. *Am J Hum Genet*. 2007;81:559-575.
39. Reich D, Price AL, Patterson N. Principal component analysis of genetic data. *Nat Genet*. 2008;40:491-492.
40. Zheng X, Shen J, Cox C, et al. HIBAG—HLA genotype imputation with attribute bagging. *Pharmacogenomics J*. 2014;14:192-200.
41. Wang C, Krishnakumar S, Wilhelmy J, et al. High-throughput, high-fidelity HLA genotyping with deep sequencing. *Proc Natl Acad Sci U S A*. 2012;109:8676-8681.
42. Thorstenson YR, Creary LE, Huang H, et al. Allelic resolution NGS HLA typing of class I and class II loci and haplotypes in Cape Town, South Africa. *Hum Immunol*. 2018;79:839-847.
43. Creary LE, Mallempati KC, Gangavarapu S, Caillier SJ, Oksenberg JR, Fernández-Viña MA. Deconstruction of HLA-DRB1*04:01:01 and HLA-DRB1*15:01:01 class II haplotypes using next-generation sequencing in European-Americans with multiple sclerosis. *Mult Scler J*. 2019;25:772-782.
44. Sempere VP, Muñiz-Castrillo S, Ambati A, et al. Human leukocyte antigen association study reveals DRB1*04:02 effects additional to DRB1*07:01 in anti-LGI1 encephalitis. *Neurol Neuroimmunol Neuroinflamm*. 2022;9:e1140.
45. Luo G, Yogeshwar S, Lin L, Mignot EJ. T cell reactivity to regulatory factor X4 in type 1 narcolepsy. *Sci Rep*. 2021;11:7841.
46. Reynisson B, Alvarez B, Paul S, Peters B, Nielsen M. NetMHCpan-4.1 and NetMHCIIpan-4.0: Improved predictions of MHC antigen presentation by concurrent motif deconvolution and integration of MS MHC eluted ligand data. *Nucleic Acids Res*. 2020;48(W1):W449-w454.
47. Wang D, Liu D, Yuchi J, et al. MusiteDeep: A deep-learning based webserver for protein post-translational modification site prediction and visualization. *Nucleic Acids Res*. 2020;48(W1):W140-W146.
48. Blom N, Gammeltoft S, Brunak S. Sequence and structure-based prediction of eukaryotic protein phosphorylation sites. *J Mol Biol*. 1999;294:1351-1362.
49. Gupta R, Brunak S. Prediction of glycosylation across the human proteome and the correlation to protein function. *Pac Symp Biocomput*. 2002;7:310-322.
50. Itoh S, Hachisuka A, Kawasaki N, et al. Glycosylation analysis of IgLON family proteins in rat brain by liquid chromatography and multiple-stage mass spectrometry. *Biochemistry*. 2008;47:10132-10154.
51. Mallajosyula V, Ganjavi C, Chakraborty S, et al. CD8+ t cells specific for conserved coronavirus epitopes correlate with milder disease in patients with COVID-19. *Sci Immunol*. 2021;6:eabg5669.
52. Wolf FA, Angerer P, Theis FJ. SCANPY: Large-scale single-cell gene expression data analysis. *Genome Biol*. 2018;19:1-5.
53. Osoegawa K, Mallempati KC, Gangavarapu S, et al. HLA alleles and haplotypes observed in 263 US families. *Hum Immunol*. 2019;80:644-660.
54. Miyadera H, Ohashi J, Lernmark Å, Kitamura T, Tokunaga K. Cell-surface MHC density profiling reveals instability of autoimmunity-associated HLA. *J Clin Invest*. 2015;125:275-291.

55. Ollila HM, Fernandez-Vina M, Mignot E. HLA-DQ allele competition in narcolepsy: A comment on Tafti et al. DQB1 locus alone explains most of the risk and protection in narcolepsy with cataplexy in Europe. *Sleep*. 2015;38:147-151.
56. Sabater L, Planagumà J, Dalmau J, Graus F. Cellular investigations with human antibodies associated with the anti-IgLON5 syndrome. *J Neuroinflammation*. 2016;13:226.
57. Hains PG, Truscott RJ. Age-dependent deamidation of lifelong proteins in the human lens. *Invest Ophthalmol Vis Sci*. 2010;51: 3107-3114.
58. Svozil J, Baerenfaller K. A cautionary tale on the inclusion of variable posttranslational modifications in database-dependent searches of mass spectrometry data. *Methods Enzymol*. 2017;586: 433-452.
59. Heo S, Diering GH, Na CH, et al. Identification of long-lived synaptic proteins by proteomic analysis of synaptosome protein turnover. *Proc Natl Acad Sci U S A*. 2018;115:E3827-E3836.
60. Nguyen H, Arribas-Layton D, Chow IT, et al. Characterizing T cell responses to enzymatically modified beta cell neoepitopes. *Front Immunol*. 2022;13:1015855.
61. Kato K, Nakayoshi T, Kurimoto E, Oda A. Mechanisms of deamidation of asparagine residues and effects of main-chain conformation on activation energy. *Int J Mol Sci*. 2020;21:7035.
62. McAdam SN, Fleckenstein B, Rasmussen IB, et al. T cell recognition of the dominant I-Ak–restricted hen egg lysozyme epitope: Critical role for asparagine deamidation. *J Exp Med*. 2001;193: 1239-1246.
63. Moss CX, Matthews SP, Lamont DJ, Watts C. Asparagine deamidation perturbs antigen presentation on class II major histocompatibility complex molecules. *J Biol Chem*. 2005;280: 18498-18503.
64. Fernández-Viña MA, Klein JP, Haagenson M, et al. Multiple mismatches at the low expression HLA loci DP, DQ, and DRB3/4/5 associate with adverse outcomes in hematopoietic stem cell transplantation. *Blood*. 2013;121:4603-4610.
65. Yamamoto F, Suzuki S, Mizutani A, et al. Capturing differential allele-level expression and genotypes of all classical HLA loci and haplotypes by a new capture RNA-seq method. *Front Immunol*. 2020;11:941.
66. Heidbreder A, Frauscher B, Mitterling T, et al. Not only sleepwalking but NREM parasomnia irrespective of the type is associated with HLA DQB1* 05: 01. *J Clin Sleep Med*. 2016;12:565-570.
67. Gaig C, Compta Y, Heidbreder A, et al. Frequency and characterization of movement disorders in anti-IgLON5 disease. *Neurology*. 2021;97:e1367-e1381.
68. Cirrito TP, Pu Z, Deck MB, Unanue ER. Deamidation of asparagine in a major histocompatibility complex–bound peptide affects T cell recognition but does not explain type B reactivity. *J Exp Med*. 2001;194:1165-1170.
69. Lehrbach NJ, Breen PC, Ruvkun G. Protein sequence editing of SKN-1A/Nrf1 by peptide:N-glycanase controls proteasome gene expression. *Cell*. 2019;177:737-750.e15.
70. Mei S, Ayala R, Ramarathinam SH, et al. Immunopeptidomic analysis reveals that deamidated HLA-bound peptides arise predominantly from deglycosylated precursors. *Mol Cell Proteomics*. 2020;19:1236-1247.
71. Need AC, Shashi V, Hitomi Y, et al. Clinical application of exome sequencing in undiagnosed genetic conditions. *J Med Genet*. 2012;49:353-361.
72. Pandey A, Adams JM, Han SY, Jafar-Nejad H. NGLY1 deficiency, a congenital disorder of deglycosylation: From disease gene function to pathophysiology. *Cells*. 2022;11:1155.
73. Yang K, Huang R, Fujihira H, Suzuki T, Yan N. N-glycanase NGLY1 regulates mitochondrial homeostasis and inflammation through NRF1. *J Exp Med*. 2018;215:2600-2616.
74. Wesseling H, Mair W, Kumar M, et al. Tau PTM profiles identify patient heterogeneity and stages of Alzheimer's disease. *Cell*. 2020;183:1699-1713.
75. Paul S, Grifoni A, Peters B, Sette A. Major histocompatibility complex binding, eluted ligands, and immunogenicity: Benchmark testing and predictions. *Front Immunol*. 2019;10: 3151.
76. Freeze HH, Kranz C. Endoglycosidase and glycoamidase release of N-linked glycans. *Curr Protoc Mol Biol*. 2010;Chapter 17:Unit 17 13A.
77. Zhou C, Osterbye T, Bach E, et al. Focused B cell response to recurring gluten motif with implications for epitope spreading in celiac disease. *Cell Rep*. 2022;41:111541.
78. Petersone L, Edner NM, Ovcinnikovs V, et al. T Cell/B cell collaboration and autoimmunity: An intimate relationship. *Front Immunol*. 2018;9:1941.
79. Koehli S, Naeher D, Galati-Fournier V, Zehn D, Palmer E. Optimal T-cell receptor affinity for inducing autoimmunity. *Proc Natl Acad Sci U S A*. 2014;111:17248-17253.
80. Martinez RJ, Evavold BD. Lower affinity T cells are critical components and active participants of the immune response. *Front Immunol*. 2015;6:468.
81. Cano-Gamez E, Soskic B, Roumeliotis TI, et al. Single-cell transcriptomics identifies an effectorness gradient shaping the response of CD4(+) T cells to cytokines. *Nat Commun*. 2020;11:1801.